Solar Wind Density Forecasting with U-Net and LSTM-based Neural Networks

Emanuele Iacobelli[1], Francesca Fiani[1] and Christian Napoli[1,2,3]

[1]Department of Computer, Control and Management Engineering, Sapienza University of Rome, 00185 Roma, Italy;
[2]Institute for Systems Analysis and Computer Science, Italian National Research Council, 00185 Roma, Italy;
[3]Department of Computational Intelligence, Czestochowa University of Technology, 42-201 Czestochowa, Poland;

Abstract

Forecasting changes in solar wind properties accurately is crucial for predicting space weather, as it significantly impacts the majority of space operations and the telecommunication system. To meet this challenge, we introduce an architecture that combines U-Net's capabilities for segmenting coronal holes from high-resolution sun images with the predictive abilities of Long Short-Term Memory (LSTM) and ConvLSTM models. This architecture predicts solar wind density using sun surface images obtained from the AIA 193 Å dataset (provided by NASA) and historical electron and proton density data from the OMNI and ELM2 datasets (also provided by NASA), covering the entire year 2012. Our findings demonstrate the system's ability to generate reliable coronal hole segmentation maps and achieve good accuracy in forecasting solar wind density.

Keywords

Solar Wind Prediction, Coronal Holes Segmentation, Machine Leaning, U-Net, Long-Short Term Memory, ConvLSTM, Space Weather

1. Introduction

The solar wind is a dynamic flow of charged particles in a plasma state, originating from the Sun's corona. This stream of particles emanated from expansive luminous areas known as coronal holes, overcomes the Sun's gravitational force thanks to its elevated thermal energy and spreads all over the universe[1]. Composed primarily of electrons and protons, this solar wind significantly influences the conditions of the entire solar system. While the Earth's magnetic field shields the majority of this wind, excessive strength can lead to geomagnetic storms that are particularly dangerous, especially for astronauts and spacecraft, and can cause disruptions in power grids, interfere with satellite communications, and even lead to notable incidents such as the 1989 blackout in Quebec caused by a high-velocity solar wind. Other historical events, like the solar storm 1859 and the Miyake event around 774-775 AD, underscore the immense impact of solar wind variations. The former disrupted telegraph communications, while the latter, studied through the analysis of Carbon 14 in the polar ice, highly surpassed the intensity of the 1859 storm. We can only imagine the consequences of such magnetic storms in today's world and the mobility of citizens [2]. In a society heavily reliant on electricity, this could significantly disrupt our daily lives. Therefore, predicting the solar wind behavior is crucial for safeguarding both our technological infrastructure and the safety of space missions, reinforcing the need for ongoing research and forecasting capabilities. For this reason, in this study, we employed a customized U-Net architecture [3, 4, 5] to segment coronal holes from high-resolution images of the sun in the AIA 193 Å dataset captured by NASA's Solar Dynamics Observatory (SDO) space telescope. Subsequently, we leveraged these segmented images along with historical solar wind properties extracted from the OMNI and ELM2 datasets to train a system, composed of LSTM-based [6, 7, 8] architectures and a feed-forward neural network, for forecasting solar wind density in terms of proton and electron densities. The decision to use binary coronal hole segmentation maps derives from our desire to evaluate the models' predictive capability for solar wind density even in the absence of detailed solar surface features.

1.1. Roadmap

This paper is organized as follows: first of all, a summary of the different types of techniques developed to predict solar wind properties is presented in Section 2. Then, the description of the dataset employed in this experiment is proposed in Section 3. Following this, a detailed explanation of the system we developed is illustrated in Section 4. Subsequently, the evaluation of our architecture is presented in Section 5. Finally, we summarized the content of the article and we outlined the possible viable improvements that can be made in Section 6.

ICYRIME 2023: 8th International Conference of Yearly Reports on Informatics, Mathematics, and Engineering. Naples, July 28-31, 2023
iacobelli@diag.uniroma1.it (E. Iacobelli); fiani@diag.uniroma1.it (F. Fiani); cnapoli@diag.uniroma1.it (C. Napoli)
0009-0003-1379-9106 (E. Iacobelli); 0000-0002-3336-5853 (C. Napoli)

2. Related Works

In the realm of works focusing on segmenting coronal holes, the field of image segmentation has experienced significant advancements in recent years, with the U-Net model emerging as a powerful, versatile, and widely adopted architecture used across various domains such as medical imaging, remote sensing, and astronomy. Originally developed for tasks like biomedical image segmentation (e.g., cell and tissue segmentation from microscopy images), the U-Net architecture features a classic encoder-decoder structure characterized by its symmetric U-shape. The encoder component typically follows a traditional CNN architecture, incorporating successive convolutional layers and pooling layers to reduce spatial dimensions while capturing high-level hierarchical features from input images. On the other hand, the decoder utilizes upsampling layers to restore the spatial resolution of feature maps. This restoration is achieved through skip connections directly linked to the encoder, enabling precise localization by providing detailed information from the original input images. In the realm of solar physics, researchers have explored adaptations of the U-Net model for segmenting solar features such as sunspots or coronal holes from high-resolution imagery. These adaptations often involve fine-tuning the network to address specific challenges presented by solar images, such as the varying intensity and appearance of sunspots against a dynamic background.

In [9, 10], the authors trained a U-Net neural network using daily SDO/AIA 193 Å solar disc images and corresponding coronal hole segmentation maps from 2010 to 2017 provided by the Kislovodsk Mountain Astronomical Station. They evaluated this model using data from 2017 to 2018 and compared it with other semi-automatic segmentation procedures. The authors found that U-Net outperformed the other algorithms used for coronal hole segmentation, demonstrating higher generalization power and accuracy.

A similar approach is presented in [11], where a customized U-Net architecture named SCSS-NET was developed to segment solar corona structures from Sun images. This system was benchmarked against established algorithms such as the Spatial Possibilistic Clustering Algorithm (SPoCA) [12], the Coronal Hole Identification via Multi-thermal Emission Recognition Algorithm (CHIMERA) [13], and the Region Growth algorithm [14]. The SCSS-NET model demonstrated promising segmentation results comparable to these methods. However, its performance is contingent upon the accuracy of reference annotations.

Regarding the different architectures introduced to solve the solar wind properties forecasting, most of them are focused on predicting the solar wind speed. For instance, in [15], a straightforward Convolutional Neural Network (CNN) architecture is employed to solve a simple regression problem that given as input a single RGB image of the Sun, predicts the corresponding solar wind speed that will be registered at the L1 point. Briefly, a CNN [16] is a network consisting of layers applying convolutional operations to detect patterns, features, or objects within images.

Another notable work was proposed by the authors of [17] that presented WindNet, a CNN-LSTM framework that uses a pre-trained GoogleNet architecture [18] as a feature extractor. In specifics, a Long Short-Tem Memory (LSTM) is an extension of a Recurrent Neural Network (RNN) [19] intended to capture and combine long- and short-term dependencies in data sequences. WindNet was created to look into the optimal combination of *delay D* and *history H* values to predict the solar wind speed.

In [20], to predict the solar wind propagation delay between the Lagrangian point L1 and the Earth, some classic machine learning methods are employed (e.g., Random Forest Regression (RF) [21], Gradient Boosting (GB) [22], and Linear Regression (as ordinary least square regression presented in [23]) and their performance is compared to classic physics models such as the flat or vector delay methods. The GB turned out to be the best model. Despite its high accuracy, the evident limitation of solving this particular problem lies in the small time interval to be predicted, a few seconds, which is the time necessary for the Solar Wind to travel from the L1 point and the Earth.

In ref. [24], linear prediction functions were used to forecast the solar wind speed at 1 AU up to four days in advance by using solar images with a 1-hour time resolution. In detail, through a thresholding process, the active areas in the central meridional slice of the Sun were extracted, as it is part of the sun that is most directly facing the Earth, and used as input to the empirical model-based.

In [25], the authors compared the performance of empirical, hybrid empirical-physics-based, and fully physics-based coupled corona-heliosphere models over 8 years of solar wind observations. They found that the empirical baseline schemes produce the "best" predictions of solar wind parameters in near-Earth space, at least in terms of the Mean Squared Error (MSE). However, even if the physics-based approaches still require some further parameterization, with continued refinement, they can potentially outperform empirical schemes in terms of prediction. This is especially true when it comes to the integration of transient structures, the drivers of major space weather disturbances.

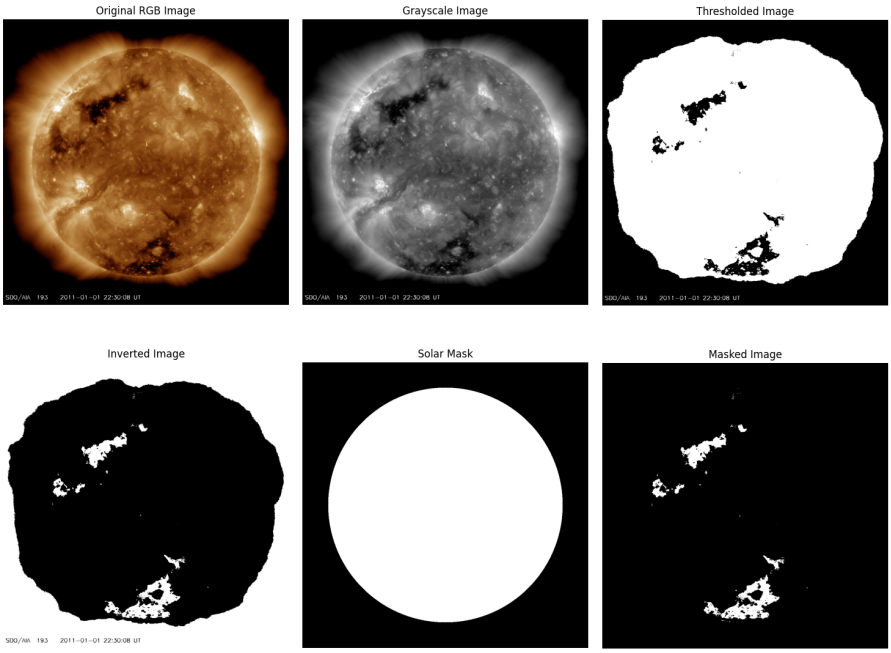

Figure 1: These images illustrate the steps of the algorithm we utilized to generate a binary coronal hole segmentation map for training our customized U-Net. Initially, we downscaled the original sun images to 256×256 and converted them to grayscale. Next, we manually selected a threshold to segment the coronal holes. Finally, we inverted the resulting images to highlight the segmented coronal holes and applied a circular mask to isolate them.

3. Dataset

We employed the AIA 193 Å dataset from NASA's Solar Dynamics Observatory (SDO) space telescope to train the U-Net architecture for coronal hole segmentation. The SDO's Atmospheric Imaging Assembly (AIA) instrument captures solar images across various ultraviolet and extreme ultraviolet wavelengths, including the 193 Ångström (Å) wavelength, crucial for studying coronal structures like coronal holes, coronal loops, and active regions.

To generate the ground truth coronal hole segmentation maps, we performed manual thresholding on all images from 2011 to 2012, with a temporal resolution of 6 hours, using the following algorithm: first, we downscaled the original high-resolution images to 256×256 pixels to balance feature detail and computational load. Next, we converted them to grayscale and manually selected a threshold to enhance coronal hole visibility. Subsequently, we inverted the binary images obtained to highlight segmented coronal holes and applied a circular mask representing the sun's shape to isolate the segmented coronal holes. The complete procedure for extracting coronal hole segmentation maps is illustrated in Fig. 1.

To train the LSTM-based models responsible for forecasting solar wind density, we created an additional dataset by combining the coronal hole segmentation maps obtained by our customized U-Net architecture with two tabular datasets. The first one is the OMNI dataset, which is an hourly resolution multi-source dataset of near-Earth solar wind's magnetic field and plasma parameters, such as the IMF (magnitude and vector), flow velocity (magnitude and vector), flow pressure, proton density, alpha particle to proton density ratio, and more. The second one is the ELM2 (EESA Low Electron Moments) dataset, which comes from the WIND 3-D Plasma experiment that makes measurements of the full 3-D distribution of suprathermal electrons and ions. Since all these datasets have coinciding timestamps, we merged the information available for the year 2012 with a time interval of 6 hours into a single dataset. It is important to highlight that while generating this dataset we make a strong approximation. Even if the solar wind speed is extremely variable, we associated the coronal hole segmentation maps with the tabular data acquired two days later.

The pre-processing of this latter dataset involved different operations. First of all, we removed the constant values from the two tabular datasets, since they do not give valuable information to the training process. Subsequently, we removed the outliers by eliminating values

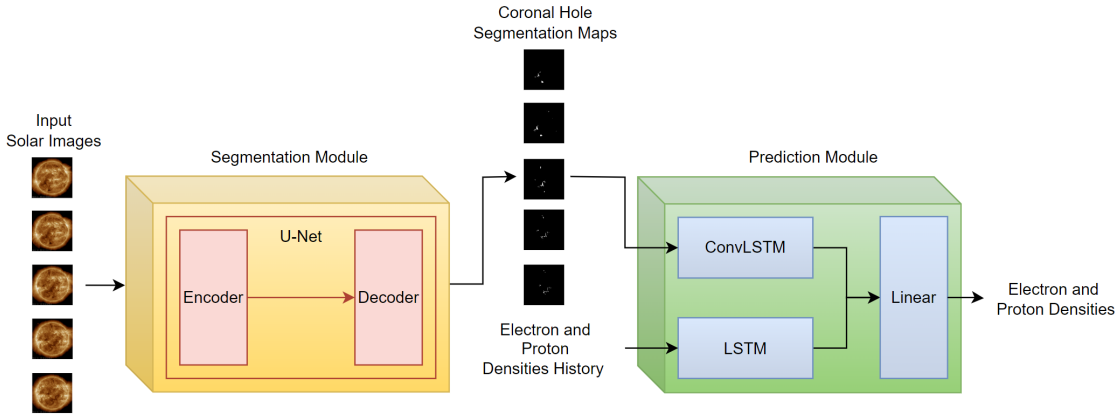

Figure 2: This image illustrates the complete pipeline of our system. The historical solar images serve as input to the Segmentation Module, generating corresponding coronal hole segmentation maps. These maps, along with the historical electron and proton density data, are then fed into the Prediction Module. Specifically, the segmentation maps go to the ConvLSTM, while the solar wind density history is given as input into the standard LSTM. Then, the ConvLSTM's output is flattened, combined with the LSTM's output, and subsequently inputted into a feed-forward neural network responsible for predicting solar wind density.

exceeding 5 times the standard deviation for each respective feature. Finally, since we had to deal with different physical quantities having different orders of magnitude, we normalized the data in the range [0,1] based on the maximum and minimum values present in the dataset for each feature.

4. Methodology

The full pipeline of our system, illustrated in Fig. 2, consists of two main modules. The segmentation module extracts the binary coronal hole segmentation maps from the history of high-resolution images of the sun. Subsequently, the prediction module forecasts solar wind density by integrating the historical coronal hole segmentation maps with the historical solar density data.

4.1. Segmentation Module

The segmentation module comprises our customized U-Net architecture. The implementation details are depicted in Fig. 3. Unlike the traditional implementation, we have incorporated residual blocks instead of convolutional blocks in the encoder. A residual block includes skip connections that enable the network to learn residual mappings. These skip connections also facilitate gradient flow, addressing the vanishing gradient problem and supporting the training of deeper models. Moreover, following each convolutional layer, we have incorporated batch normalization and dropout layers (with a dropout rate of 0.3). Finally, we have opted to use the Leaky ReLU activation function instead of the traditional ReLU to better handle the vanishing gradient problem and enhance training stability.

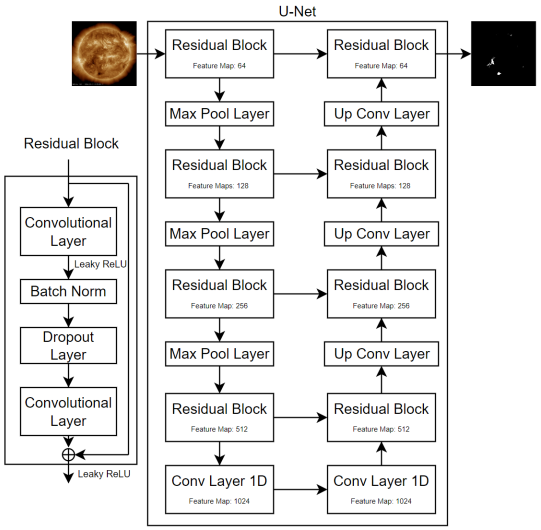

Figure 3: This image showcases our customized U-Net architecture. We replaced Convolutional Layers with Residual Blocks and included Batch Normalization and Dropout Layers after each Convolutional Layer. Moreover, we chose to use Leaky ReLU instead of the standard ReLU activation function to improve the network's training.

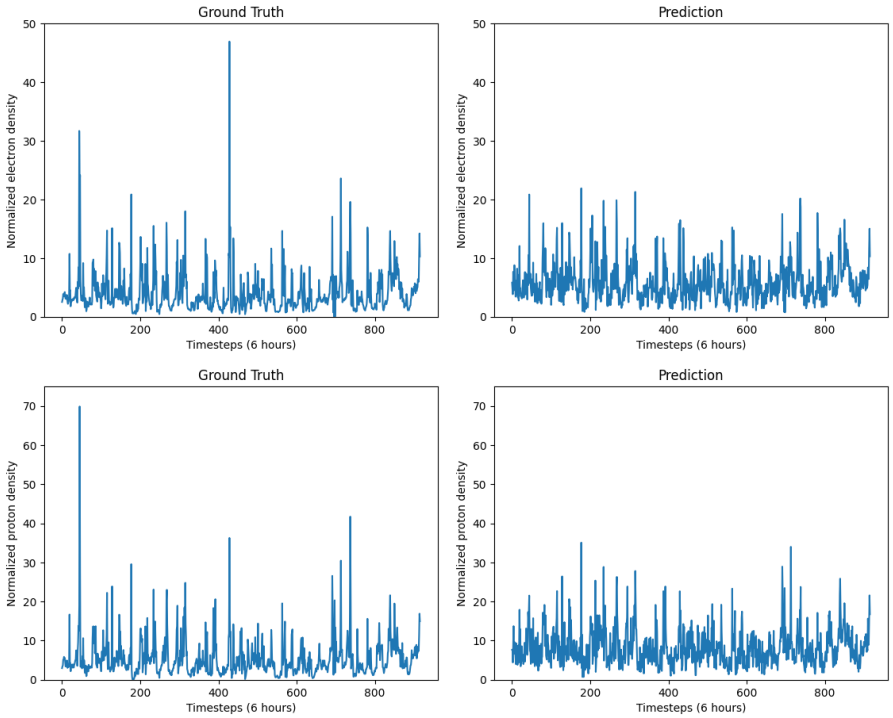

Figure 4: The top two images represent the ground truth (left) and predictions (right) of our system for electron density over a 225-day time interval, with measurements taken every 6 hours. The images below display the ground truth (left) and predictions of the proton density during the same period.

4.2. Prediction Module

The LSTMs and their variants stand out as the most widely utilized architectures for learning from sequential data and forecasting future states. LSTMs excel in analyzing the evolution of coronal holes over time, effectively handling the nonlinear and unpredictable aspects of their movement and morphological changes. Consequently, the prediction module incorporates two networks: a ConvLSTM architecture for analyzing historical binary coronal hole segmentation maps and a standard LSTM architecture for processing historical solar wind density data. We have stacked five layers for both of these networks and included dropout layers (with a dropout rate of 0.1) after each LSTM layer except the last one. To predict electron and proton densities, we flattened the output of the ConvLSTM and concatenated it with the output of the standard LSTM. This combined output is then passed through a linear feed-forward neural network, composed of three linear layers, responsible for the outcome of our system.

5. Results

For validating our segmentation module, we employed two types of error functions: the Intersection over Union (IoU) and the Dice coefficient. The IoU measures the overlap between the predicted segmentation and the ground truth divided by the union:

$$IoU = \frac{TP}{TP + FP + FN} \tag{1}$$

The Dice coefficient, also known as F1 score, is a statistical tool that measures the similarity between two sets of data:

$$Dice = \frac{2TP}{2TP + FP + FN} \tag{2}$$

Here, TP (true positive) represents correctly segmented pixels, FP (false positive) denotes predicted object mask pixels not matching the ground truth, and FN (false negative) indicates ground truth object mask pixels not associated with predicted pixels.

Based on these error metrics, our segmentation model has demonstrated excellent performance, achieving an IoU of 0.93 and a Dice score of 0.95.

Regarding the prediction module instead, we leveraged the Mean Squared Error (MSE) function and we achieved a value of 15.29.

An example of the prediction capabilities of our system is shown in Fig. 4.

6. Conclusion

In this study, we have developed and evaluated a comprehensive approach for forecasting solar wind density, addressing the critical need for accurate space weather predictions. Our system distinguishes itself for the balance between computation load and the very high precision in accurately segmenting coronal holes from high-resolution sun images and the good forecasting capabilities of the prediction module that effectively combines the LSTM and ConvLSTM networks. Moving forward, we propose future improvements by substituting the convolutional layers with Vision Transformers [26, 27, 28]. This enhancement strategy aims to further elevate the accuracy and robustness of our system, paving the way for more precise solar wind density forecasts and improved space weather predictions. Furthermore, another improvement to enhance the performance of our system involves expanding the dataset used to train our customized U-Net architecture. Specifically, we aim to increase the volume of manually generated coronal hole segmentation maps within the dataset. By incorporating a more extensive and diverse dataset, we anticipate boosting the generability power of the network. This expansion strategy is expected to enable the neural network to generalize better to unseen data and variations in coronal hole structures. Improved generalization can also benefit the prediction module by achieving better results and reducing forecasting errors.

Acknowledgments

This work has been developed at is.Lab() Intelligent Systems Laboratory at the Department of Computer, Control, and Management Engineering, Sapienza University of Rome (https:// islab.diag.uniroma1.it). The work has also been partially supported from Italian Ministerial grant PRIN 2022 "ISIDE: Intelligent Systems for Infrastructural Diagnosis in smart-concretE", n. 2022S88WAY - CUP B53D2301318, and by the Age-It: Ageing Well in an ageing society project, task 9.4.1 work package 4 spoke 9, within topic 8 extended partnership 8, under the National Recovery and Resilience Plan (PNRR), Mission 4 Component 2 Investment 1.3—Call for tender No. 1557 of 11/10/2022 of Italian Ministry of University and Research funded by the European Union—NextGenerationEU, CUP B53C22004090006.

References

[1] F. Bonanno, G. Capizzi, A. Gagliano, C. Napoli, Optimal management of various renewable energy sources by a new forecasting method, 2012, pp. 934 – 940. doi:10.1109/SPEEDAM.2012.6264603.

[2] N. Brandizzi, S. Russo, G. Galati, C. Napoli, Addressing vehicle sharing through behavioral analysis: A solution to user clustering using recency-frequency-monetary and vehicle relocation based on neighborhood splits, Information (Switzerland) 13 (2022). doi:10.3390/info13110511.

[3] O. Ronneberger, P. Fischer, T. Brox, U-net: Convolutional networks for biomedical image segmentation, in: Medical image computing and computer-assisted intervention–MICCAI 2015: 18th international conference, Munich, Germany, October 5-9, 2015, proceedings, part III 18, Springer, 2015, pp. 234–241.

[4] N. N. Dat, V. Ponzi, S. Russo, F. Vincelli, Supporting impaired people with a following robotic assistant by means of end-to-end visual target navigation and reinforcement learning approaches, volume 3118, 2021, pp. 51 – 63.

[5] G. De Magistris, R. Caprari, G. Castro, S. Russo, L. Iocchi, D. Nardi, C. Napoli, Vision-based holistic scene understanding for context-aware human-robot interaction 13196 LNAI (2022) 310 – 325. doi:10.1007/978-3-031-08421-8_21.

[6] S. Hochreiter, J. Schmidhuber, Long short-term memory, Neural computation 9 (1997) 1735–1780.

[7] V. Ponzi, S. Russo, V. Bianco, C. Napoli, A. Wajda, Psychoeducative social robots for an healthier lifestyle using artificial intelligence: a case-study, volume 3118, 2021, pp. 26 – 33.

[8] X. Shi, Z. Chen, H. Wang, D.-Y. Yeung, W.-K. Wong, W.-c. Woo, Convolutional lstm network: A machine learning approach for precipitation nowcasting, Advances in neural information processing systems 28 (2015).

[9] E. A. Illarionov, A. G. Tlatov, Segmentation of coronal holes in solar disc images with a convolutional neural network, Monthly Notices of the Royal Astronomical Society 481 (2018) 5014–5021.

[10] S. Pepe, S. Tedeschi, N. Brandizzi, S. Russo, L. Iocchi, C. Napoli, Human attention assessment using a machine learning approach with gan-based data augmentation technique trained using a custom dataset, OBM Neurobiology 6 (2022). doi:10.21926/obm.neurobiol.2204139.

[11] Š. Mackovjak, M. Harman, V. Maslej-Krešňáková, P. Butka, Scss-net: solar corona structures segmentation by deep learning, Monthly Notices of the Royal Astronomical Society 508 (2021) 3111–3124.

[12] C. Verbeeck, V. Delouille, B. Mampaey, R. De Viss-

cher, The spoca-suite: Software for extraction, characterization, and tracking of active regions and coronal holes on euv images, Astronomy & Astrophysics 561 (2014) A29.
[13] T. M. Garton, P. T. Gallagher, S. A. Murray, Automated coronal hole identification via multi-thermal intensity segmentation, Journal of Space Weather and Space Climate 8 (2018) A02.
[14] A. Tlatov, K. Tavastsherna, V. Vasil'eva, Coronal holes in solar cycles 21 to 23, Solar Physics 289 (2014) 1349–1358.
[15] H. Raju, S. Das, Cnn-based deep learning model for solar wind forecasting, Solar Physics 296 (2021) 134.
[16] S. Albawi, T. A. Mohammed, S. Al-Zawi, Understanding of a convolutional neural network, in: 2017 international conference on engineering and technology (ICET), Ieee, 2017, pp. 1–6.
[17] V. Upendran, M. C. Cheung, S. Hanasoge, G. Krishnamurthi, Solar wind prediction using deep learning, Space Weather 18 (2020) e2020SW002478.
[18] C. Szegedy, W. Liu, Y. Jia, P. Sermanet, S. Reed, D. Anguelov, D. Erhan, V. Vanhoucke, A. Rabinovich, Going deeper with convolutions, in: Proceedings of the IEEE conference on computer vision and pattern recognition, 2015, pp. 1–9.
[19] R. M. Schmidt, Recurrent neural networks (rnns): A gentle introduction and overview, arXiv preprint arXiv:1912.05911 (2019).
[20] C. Baumann, A. E. McCloskey, Timing of the solar wind propagation delay between l1 and earth based on machine learning, Journal of Space Weather and Space Climate 11 (2021) 41.
[21] L. Breiman, Random forests, Machine learning 45 (2001) 5–32.
[22] J. H. Friedman, Greedy function approximation: a gradient boosting machine, Annals of statistics (2001) 1189–1232.
[23] F. Pedregosa, G. Varoquaux, A. Gramfort, V. Michel, B. Thirion, O. Grisel, M. Blondel, P. Prettenhofer, R. Weiss, V. Dubourg, et al., Scikit-learn: Machine learning in python, the Journal of machine Learning research 12 (2011) 2825–2830.
[24] T. Rotter, A. Veronig, M. Temmer, B. Vršnak, Real-time solar wind prediction based on sdo/aia coronal hole data, Solar Physics 290 (2015) 1355–1370.
[25] M. Owens, H. E. Spence, S. McGregor, W. Hughes, J. Quinn, C. Arge, P. Riley, J. Linker, D. Odstrcil, Metrics for solar wind prediction models: Comparison of empirical, hybrid, and physics-based schemes with 8 years of l1 observations, Space Weather 6 (2008).
[26] A. Alfarano, G. De Magistris, L. Mongelli, S. Russo, J. Starczewski, C. Napoli, A novel convmixer transformer based architecture for violent behavior detection 14126 LNAI (2023) 3 – 16. doi:10.1007/978-3-031-42508-0_1.
[27] A. Dosovitskiy, L. Beyer, A. Kolesnikov, D. Weissenborn, X. Zhai, T. Unterthiner, M. Dehghani, M. Minderer, G. Heigold, S. Gelly, et al., An image is worth 16x16 words: Transformers for image recognition at scale, arXiv preprint arXiv:2010.11929 (2020).
[28] G. De Magistris, M. Romano, J. Starczewski, C. Napoli, A novel dwt-based encoder for human pose estimation, volume 3360, 2022, pp. 33 – 40.